Single color and single flavor color superconductivity

Mark G. Alford,[1] Jeffrey A. Bowers,[2] Jack M. Cheyne,[1] and Greig A. Cowan[1]
[1]*Physics and Astronomy Department, Glasgow University, Glasgow, G12 8QQ, United Kingdom*
[2]*Center for Theoretical Physics, Massachusetts Institute of Technology, Cambridge, Massachusetts 02139*
(Received 25 October 2002; published 28 March 2003)

We survey the nonlocked color-flavor-spin channels for quark-quark (color superconducting) condensates in QCD, using a Nambu–Jona-Lasinio model. We also study isotropic quark-antiquark (mesonic) condensates. We make mean-field estimates of the strength and sign of the self-interaction of each condensate, using four-fermion interaction vertices based on known QCD interactions. For the attractive quark pairing channels, we solve the mean-field gap equations to obtain the size of the gap as a function of quark density. We also calculate the dispersion relations for the quasiquarks, in order to see how fully gapped the spectrum of fermionic excitations will be. We use our results to specify the likely pairing patterns in neutral quark matter, and comment on possible phenomenological consequences.

DOI: 10.1103/PhysRevD.67.054018 PACS number(s): 12.38.−t, 11.15.Ex, 24.85.+p

I. INTRODUCTION

It is well known by now that the BCS mechanism that underlies superconductivity in metals is likely to operate even more strongly in dense quark matter [1–5] (for reviews, see Ref. [6]). Generally, pairing between quarks of different flavors has received the most attention. This is because the strongest attractive interaction occurs in the color-antisymmetric spin-zero channel; therefore, by Fermi statistics the flavor wave function must be antisymmetric, involving two different flavors. This is the pattern of pairing in the heavily studied ''two-flavor color superconducting'' (2SC) [4,5] and ''color-flavor-locked'' (CFL) [7] phases of quark matter. However, there is strong reason to believe that these are not the only pairing patterns that are relevant in nature, and in this paper we survey and discuss some of the channels that are available to quarks that cannot participate in 2SC or CFL pairing.

The essence of the BCS mechanism is that a Fermi surface is unstable against pairing if there are any fermion-fermion channels in which the interaction is attractive [8]. For electrons in metals this condition is met only where phonon-mediated attraction overwhelms Coulomb repulsion. But there are certainly channels in which the dominant QCD quark-quark interaction is attractive, as indicated by the fact that a low density and temperature quarks bind strongly together to form hadrons. Mean-field calculations using QCD-inspired Nambu–Jona-Lasinio (NJL) models [7,9–12], lattice studies of NJL models [13], and calculations using gluon exchange with a hard dense loop resummed gluon propagator [14–18] confirm this, and indicate that the main pairing patterns are pure CFL for light strange quarks, with possible kaon condensation (CFL-K^0) for intermediate mass strange quarks, and 2SC+s for heavier strange quarks. However, these calculations do not take into account the requirement of electric and color neutrality, which must be obeyed in uniform dense matter in the real world, such as might be found in the core of a compact star.

The effects of imposing neutrality were recently studied in a model-independent expansion in powers of m_s/μ [19], and in preliminary Nambu–Jona-Lasinio model calculations [20]. Those calculations indicate that the 2SC+s phase suffers a significant penalty for remaining neutral, and may not occupy such a large part of the phase diagram as previously thought.

A conjectured phase diagram is sketched in Fig. 1, where we show schematically the regions of phase space in which various phases, each breaking a particular set of symmetries, are expected to exist. The diagram shows the m_s-μ plane at temperature $T=0$, and the u and d quark masses are set to zero.

At low strange quark mass ($m_s \ll m_s^{\rm cont}$), compression of nuclear matter leads to the production of hyperons (the ''strange hadronic phase''), and then a transition into an isospin-symmetric phase which by quark-hadron continuity [21] can be interpreted as a particular pairing pattern of baryons or as quark matter in the chiral symmetry breaking color-flavor-locked phase.

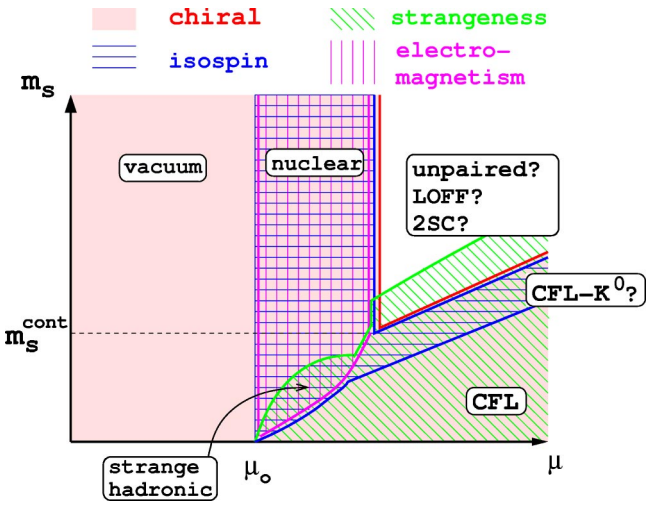

FIG. 1. A conjectured phase diagram for neutral dense matter at zero temperature as a function of quark chemical potential μ and strange quark mass m_s according to Ref. [19]. The up and down quark masses are assumed zero. The symmetries broken by the various phases are indicated by the different shading styles. The phase structure in the chirally unbroken wedge in the upper right hand corner is still uncertain, and is the topic of this paper.

At slightly higher strange quark mass, compression of strange hadronic matter may lead to an isospin broken phase that can be interpreted as hyperonic matter with Σ^0 pairing [22] or as color-flavor-locked quark matter with K^0 condensation [23]. However, the existence of this phase at these densities is uncertain because of possibly large instanton effects [24].

At high strange quark mass ($m_s > m_s^{\rm cont}$) color-flavor locking is pushed to higher densities, and there is an interval of densities where we expect non-color-flavor-locked quark matter to exist. This is the wedge in the upper right part of the m_s-μ plane (Fig. 1) where chiral symmetry is restored. (In the figure it is assumed that close to the transition to CFL or CFL-K^0 there will be some strange quarks present, and they will pair somehow, breaking strangeness.) We are uncertain of the favored phase(s) in that region.

Since only the color-flavor-locked phases pair all the momentum modes of all the quark colors and flavors, it seems that the upper-right wedge region will involve phases that leave some species of quark unpaired. However, the BCS argument implies that the supposedly unpaired quarks will seek *some* attractive channel in which to pair, and in this paper we study some of the possibilities. This question is of direct relevance to compact star physics, where the smallest gap controls transport properties such as the specific heat and neutrino emission rate. The density of a compact star rises from nuclear density near the surface to a much higher but as yet unknown value in the core, so unless there is a direct transition from nuclear to color-flavor-locked quark matter, there will be regions where some sort of single color or flavor pairing is likely.

Imposing electrical neutrality and equilibrium under the weak interactions tends to split apart the Fermi momenta of the different flavors. We therefore expect that the general scenarios for matter in the non-color-flavor-locked region are the following: (1) There may be no BCS pairing of different flavors [19], so the quarks of each flavor must find some channel in which to pair with themselves; (2) as the calculation of Ref. [20] suggests, there may be some 2SC+s pairing, i.e., a phase that involves BCS pairing the u and d quarks of two colors (red and green, say), leaving all the s quarks and the blue u and d quarks to find other pairing channels; (3) all nine colors and flavors could pair in a non-BCS fashion, involving only a subset of their momentum modes. This is crystalline or Larkin-Ovchinnikov-Fulde-Ferrell (LOFF) pairing [25–27], in which species whose Fermi surfaces are too far apart to support standard translationally invariant BCS pairing instead form pairs with net momentum, utilizing only part of their Fermi surfaces, and breaking translational invariance.

In this paper we will explore possible single color or single flavor pairing channels that could arise in scenarios 1 and 2. We will study translationally invariant, but not necessarily isotropic, pairing [3,4,28,29]. Such phases may have nonzero angular momentum, spontaneously breaking rotational invariance. In the following sections we survey the nonlocked quark pairing channels, paying particular attention to the single flavor and/or single color channels. We identify the attractive channels using NJL models with four-fermion interactions based on instantons, magnetic gluons, and combined electric and magnetic gluons. For the attractive channels we solve the gap equations, deduce the quasiquark spectrum, and comment on possible physical manifestations. Finally, we perform a similar survey of mesonic channels, in which exotic pairing has been posited [30].

II. MEAN-FIELD SURVEY OF QUARK PAIRING CHANNELS

A. Calculation

To see which channels are attractive we perform a mean-field calculation of the pairing energy for a wide range of condensation patterns. We write the NJL Hamiltonian in the form

$$H = H_{\rm free} + H_{\rm interaction},$$

$$H_{\rm free} = \bar{\psi}(\partial\!\!\!/ - \mu\gamma_0 + m)\psi, \tag{2.1}$$

$$H_{\rm interaction} = \psi^{\dagger ia}_{\alpha}\psi^{\beta b}_{j}\psi^{\dagger kc}_{\gamma}\psi^{\delta d}_{l}\mathcal{H}^{\alpha\ \ j\ \ \gamma\ \ l}_{ia\ \ \beta b\ \ kc\ \ \delta d},$$

where color indices are $\alpha,\beta,\gamma,\delta$, flavor indices are i,j,k,l, and spinor indices are a,b,c,d. The four-fermion interaction is supposed to be a plausible model of QCD, so in the interaction kernel $\mathcal{H}$ we include three terms, with the color-flavor-spinor structure of a two-flavor instanton, electric gluon exchange, and magnetic gluon exchange,

$$\mathcal{H} = \mathcal{H}_{\rm elec} + \mathcal{H}_{\rm mag} + \mathcal{H}_{\rm inst},$$

$$\mathcal{H}_{\rm elec} = \tfrac{3}{8}G_E\delta^j_i\delta^l_k\delta_{ab}\delta_{cd}\tfrac{2}{3}(3\delta^\alpha_\delta\delta^\gamma_\beta - \delta^\alpha_\beta\delta^\gamma_\delta),$$

$$\mathcal{H}_{\rm mag} = \tfrac{3}{8}G_M\delta^j_i\delta^l_k\sum_{n=1}^{3}[\gamma_0\gamma_n]_{ab}[\gamma_0\gamma_n]_{cd} \times\tfrac{2}{3}(3\delta^\alpha_\delta\delta^\gamma_\beta - \delta^\alpha_\beta\delta^\gamma_\delta), \tag{2.2}$$

$$\mathcal{H}_{\rm inst} = -\tfrac{3}{4}G_I\varepsilon_{ik}\varepsilon^{jl}\tfrac{1}{4}\{[\gamma_0(1+\gamma_5)]_{ab}[\gamma_0(1+\gamma_5)]_{cd} + [\gamma_0(1-\gamma_5)]_{ab}[\gamma_0(1-\gamma_5)]_{cd}\} \times\tfrac{2}{3}(3\delta^\alpha_\beta\delta^\gamma_\delta - \delta^\alpha_\delta\delta^\gamma_\beta).$$

We consider condensates that factorize into separate color, flavor, and Dirac tensors (i.e., that do not show ''locking'') and calculate their binding energy by contracting them with Eq. (2.2).

There is no Fierz-type ambiguity in this procedure. For a given pairing pattern X, the condensate is

$$\langle\psi^{\beta b}_j\psi^{\delta d}_l\rangle_{\rm 1PI} = \Delta(X)\mathfrak{C}^{\beta\delta}_{(X)}\mathfrak{F}_{(X)jl}\Gamma^{bd}_{(X)}. \tag{2.3}$$

We can then calculate the interaction (''binding'') energy of the various condensates,

$$H = -\sum_X \Delta(X)^2(S^{(X)}_{\rm elec}G_E + S^{(X)}_{\rm mag}G_M + S^{(X)}_{\rm inst}G_I). \tag{2.4}$$

TABLE I. Binding strengths of diquark channels in NJL models in the mean-field approximation. The first six columns specify the channels, and the last three columns give their attractiveness in NJL models with various types of four-fermion vertex: two-flavor instanton, single gluon exchange, single magnetic gluon exchange (expected to dominate at higher density). See Eqs. (2.3) and (2.4) and subsequent explanation.

Structure of condensate						Binding strength		
							Gluon	
Color	Flavor	j	Parity	Dirac	BCS enhancement	Instanton S_{inst}	Full $S_{\text{elec}}+S_{\text{mag}}$	Magnetic only S_{mag}
$\overline{\mathbf{3}}_A$	$\mathbf{1}_A$	0_A	+	$C\gamma_5$ LL	$\mathcal{O}(1)$	+64	+64	+48
$\overline{\mathbf{3}}_A$	$\mathbf{1}_A$	0_A	−	C LL	$\mathcal{O}(1)$	−64	+64	+48
$\overline{\mathbf{3}}_A$	$\mathbf{1}_A$	0_A	+	$C\gamma_0\gamma_5$ LR	$\mathcal{O}(m)$	0	−32	−48
$\overline{\mathbf{3}}_A$	$\mathbf{1}_A$	1_A	−	$C\gamma_3\gamma_5$ LR	$\mathcal{O}(1)$	0	+32	+16
$\mathbf{6}_S$	$\mathbf{1}_A$	1_S	−	$C\sigma_{03}\gamma_5$ LL	$\mathcal{O}(1)$	−16	0	+4
$\mathbf{6}_S$	$\mathbf{1}_A$	1_S	+	$C\sigma_{03}$ LL	$\mathcal{O}(1)$	+16	0	+4
$\mathbf{6}_S$	$\mathbf{1}_A$	0_S	−	$C\gamma_0$ LR	0	0	+8	+12
$\mathbf{6}_S$	$\mathbf{1}_A$	1_S	+	$C\gamma_3$ LR	$\mathcal{O}(1)$	0	−8	−4
$\overline{\mathbf{3}}_A$	$\mathbf{3}_S$	1_S	−	$C\sigma_{03}\gamma_5$ LL	$\mathcal{O}(1)$	0	0	−16
$\overline{\mathbf{3}}_A$	$\mathbf{3}_S$	1_S	+	$C\sigma_{03}$ LL	$\mathcal{O}(1)$	0	0	−16
$\overline{\mathbf{3}}_A$	$\mathbf{3}_S$	0_S	−	$C\gamma_0$ LR	0	0	−32	−48
$\overline{\mathbf{3}}_A$	$\mathbf{3}_S$	1_S	+	$C\gamma_3$ LR	$\mathcal{O}(1)$	0	+32	+16
$\mathbf{6}_S$	$\mathbf{3}_S$	0_A	+	$C\gamma_5$ LL	$\mathcal{O}(1)$	0	−16	−12
$\mathbf{6}_S$	$\mathbf{3}_S$	0_A	−	C LL	$\mathcal{O}(1)$	0	−16	−12
$\mathbf{6}_S$	$\mathbf{3}_S$	0_A	+	$C\gamma_0\gamma_5$ LR	$\mathcal{O}(m)$	0	+8	+12
$\mathbf{6}_S$	$\mathbf{3}_S$	1_A	−	$C\gamma_3\gamma_5$ LR	$\mathcal{O}(1)$	0	−8	−4

The binding strengths $S^{(X)}_{\text{interaction}}$ give the strength of the self-interaction of the condensate X due to the specified part of the interaction Hamiltonian.

B. Properties of the pairing channels

In Table I we list the the simple (translationally invariant, factorizable) channels available for quark pairing. The meanings of the columns are as follows.

(1) *Color*. Two quarks make either an antisymmetric color triplet (which requires quarks of two different colors) or a symmetric sextet (which can occur with quarks of two different colors, and also if both quarks have the same color). For the $\overline{\mathbf{3}}_A$ we use $\mathfrak{C}^{\beta\delta}=\varepsilon^{\beta\delta}$ in Eq. (2.3). For the $\mathbf{6}_S$ we use a single color representative $\mathfrak{C}^{\beta\delta}=\delta^{\beta,1}\delta^{\delta,1}$ in Eq. (2.3).

(2) *Flavor*. Two quarks make either an antisymmetric flavor singlet (which requires quarks of two different flavors) or a symmetric triplet (which can occur with quarks of two different flavors, and also if both quarks have the same flavor). For the $\mathbf{1}_A$ we use $\mathfrak{F}_{jl}=\sigma^2_{jl}$ and for the $\mathbf{3}_S$ we use $\mathfrak{F}_{jl}=\sigma^1_{jl}$ in Eq. (2.3).

(3) *Spin, parity*. Since the chemical potential explicitly breaks the Lorentz group down to three-dimensional rotations and translations, it makes sense to classify condensates by their total angular momentum quantum number j and parity.

(4) *Dirac*. This column gives the Dirac matrix structure Γ^{bd} used in Eq. (2.3), so the condensate is $\psi^T\Gamma\psi$. We also designate each condensate as "LL" (even number of gamma matrices, so pairs same-chirality quarks) or "LR" (odd number of gamma matrices, so pairs opposite-chirality quarks).

(5) *BCS enhancement*. Condensates that correspond to pairs of particles or holes near the Fermi surface have a BCS singularity in their gap equation that guarantees a solution, no matter how weak the coupling. To see which condensates have such a BCS enhancement, we expanded the field operators in terms of creation and annihilation operators (see Appendix C). The order of the coefficient of the $a(\mathbf{p})a(-\mathbf{p})$ and $b^\dagger(\mathbf{p})b^\dagger(-\mathbf{p})$ terms is given in the table. $\mathcal{O}(1)$ means BCS enhanced, 0 means not BCS enhanced. In the $C\gamma_0\gamma_5$ condensate the coefficient goes to zero as the quark mass goes to zero [hence it is labeled "$\mathcal{O}(m)$" in the table] meaning that the channel loses its BCS enhancement in the chiral limit. This is discussed further in Appendix C.

(6) *Binding strength*. For each channel we show the binding strength for the instanton interaction, the full (electric plus magnetic) gluon, which could reasonably be used at medium density, and for the magnetic gluon alone, which is known to dominate at ultrahigh density [31,14]. Channels with a positive binding strength and BCS enhancement will always support pairing (the gap equation always has a solution, however weak the couplings G_I, G_E, G_M). Other things being equal, the pairing with the largest binding strength will have the lowest free energy, and is the one that will actually occur.

It may seem strange that there are entries in the table with angular momentum $j=1$ and an antisymmetric Dirac structure ($C\gamma_3\gamma_5$), and with $j=0$ but a symmetric Dirac structure

$(C\gamma_0)$. If all the angular momentum came from spin this would be impossible. But even though there are no explicit spatial derivatives in the diquark operators, there can still be orbital angular momentum. In Appendix C the angular momentum content of the particle-particle component of the condensates is analyzed into its spin and orbital content. We see, for example, that $C\gamma_3\gamma_5$ has an antisymmetric space wave function $(l=1)$ and a symmetric spin wave function $(s=1)$, combined to give an antisymmetric $j=1$.

C. Results

The results of the binding strength calculation are shown in Table I. The first block is antisymmetric in flavor and color, and so describes pairing of two flavors and two colors. The second block is for two flavors and one color, the third for one flavor and two colors, and the final block for one color and one flavor.

Certain features can be easily understood: The flavor-symmetric condensates all have zero instanton binding energy, because the instanton vertex is flavor antisymmetric in the incoming quarks. The gluonic vertices give the same results for $C\gamma_5$ as for C, and for $C\sigma_{03}\gamma_5$ as for $C\sigma_{03}$, because the gluonic interaction is invariant under $\mathrm{U}(1)_A$ transformations, under which the LL condensates transform into each other $(C\gamma_5 \rightleftharpoons C$ and $C\sigma_{03}\gamma_5 \rightleftharpoons C\sigma_{03})$ while the LR condensates are invariant. We see that there are many attractive channels.

(1) Two colors and two flavors $(\bar{\mathbf{3}}_A, \mathbf{1}_A, \ldots)$. The strongly attractive channel $(\bar{\mathbf{3}}_A, \mathbf{1}_A, 0, +)(C\gamma_5)$ is the 2SC and CFL quark Cooper pairing pattern, and has been extensively studied. The gap is large enough that even species with different masses, whose Fermi momenta are quite far apart, can pair (hence the CFL phase which pairs red and green u and d, red and blue u and s, and green and blue d and s in this channel). Its parity partner $(\bar{\mathbf{3}}_A, \mathbf{1}_A, 0, -)(C)$ is disfavored by instantons, and is therefore unlikely to occur at phenomenologically interesting densities. The additional channel $(\bar{\mathbf{3}}_A, \mathbf{1}_A, 1, -)(C\gamma_3\gamma_5)$ is more weakly attractive and also breaks rotational invariance, and is therefore expected to be even less favored. This is confirmed by gap equation calculations (Fig. 2) which show that its gap is smaller by a factor of 10–100.

(2) One color, two flavors $(\mathbf{6}_S, \mathbf{1}_A, \ldots)$. It is generally emphasized that the quark-quark interaction is attractive in the color-antisymmetric $\bar{\mathbf{3}}_A$ channel. But, as we see in Table I, the color-symmetric $(\mathbf{6}_S, \mathbf{1}_A, 1, +)(C\sigma_{03})$ is attractive for instantons and the magnetic gluon four-fermion interaction. The instanton gives it a gap of order 1 MeV (Fig. 3), while the gluon interaction gives a small gap of order 1 eV (Fig. 2). This channel was originally suggested for pairing of the blue up and down quarks that are left out of 2SC [4], and is discussed in more detail in Ref. [29]. Its gap is small, so it could only pair quarks of similar mass, i.e., the light quarks, but in a real-world uniform phase such pairing will not occur either, because charge neutrality causes the up and down chemical potentials (and hence Fermi momenta) to differ by tens of MeV, which is larger than the gap. In a nonuniform mixture of two locally charged phases [32], however, it is conceivable that the up and down Fermi momenta could be similar enough to allow pairing in this channel. The parity partner $(\mathbf{6}_S, \mathbf{1}_A, 1, -)(C\sigma_{03}\gamma_5)$ is disfavored by instantons. The channel $(\mathbf{6}_S, \mathbf{1}_A, 0, -)(C\gamma_0)$ is attractive, but has no particle-particle component, and presumably only occurs for sufficiently strong coupling. Solving the gap equations for reasonable coupling strength, we find no gap in this channel.

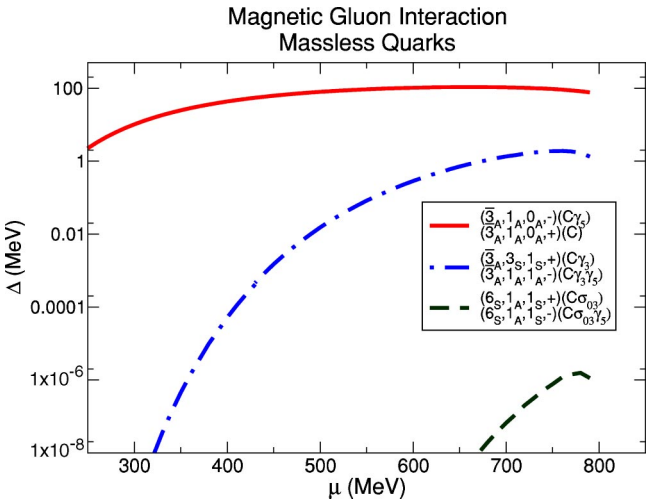

FIG. 2. Gap parameters in the attractive channels for a NJL interaction based on magnetic-gluon exchange. We show the one-flavor and two-flavor channels, for massless quarks. The cutoff is $\Lambda = 800$ MeV.

(3) Two colors and one flavor $(\bar{\mathbf{3}}_A, \mathbf{3}_S, \ldots)$. The only attractive channel is $(\bar{\mathbf{3}}_A, \mathbf{3}_S, 1, +)(C\gamma_3)$. This is a pairing option for red and green strange quarks in $2\mathrm{SC}+s$. We have solved the relevant gap equation (Figs. 2 and 4) and find gaps in the range 2–10 MeV. If three colors are available then a competing possibility is to lock the colors to the spin

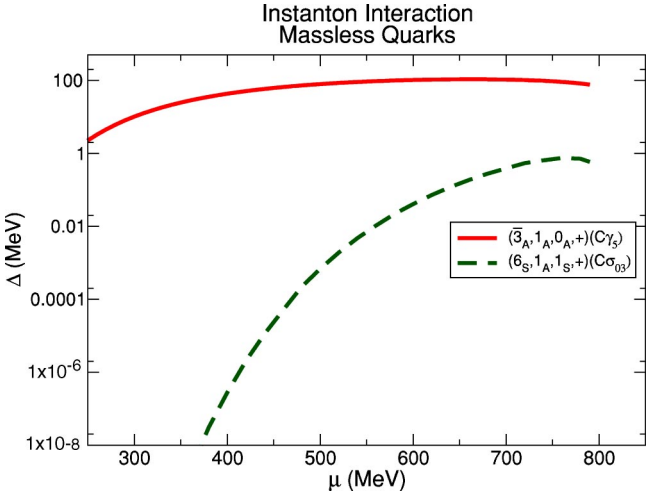

FIG. 3. Gap parameters in the attractive channels for a NJL interaction based on the two-flavor instanton. Since the instanton interaction requires two quark flavors, we take the quarks to be massless, which is a good approximation for the u and d. The cutoff is $\Lambda = 800$ MeV.

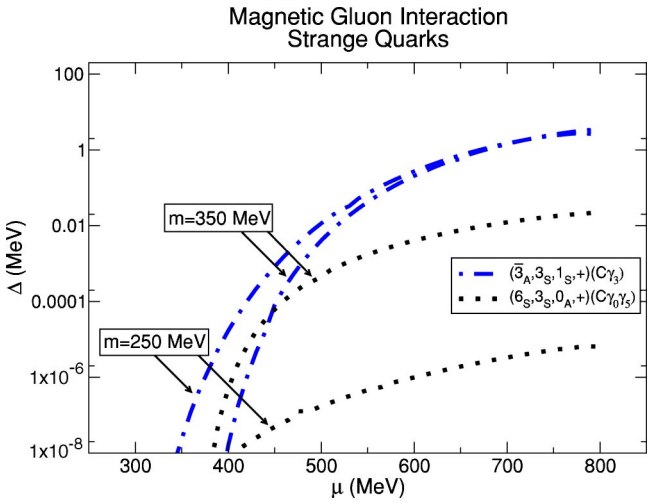

FIG. 4. Gap parameters in the attractive channels for a NJL interaction based on magnetic-gluon exchange, for quarks of mass 250 and 350 MeV, a reasonable range of values for the strange quark at medium density. We show only the single flavor channels. The cutoff is $\Lambda = 800$ MeV.

(CSL), so the condensate is a linear combination of $C\gamma_i$ and $C\sigma_{0i}$ with a color structure that is correlated with the spatial direction, e.g., red and green quarks pair in the z direction, red and blue in the y direction, and green and blue in the x direction. This leaves an unbroken global SO(3) of spatial rotations combined with color rotations, so the gap is isotropic, which helps to lower the free energy [28,33]. Note also that the channels $(\bar{\mathbf{3}}_A,\mathbf{3}_S,1,+)(C\sigma_{03})$ and $(\bar{\mathbf{3}}_A,\mathbf{3}_S,1,-)(C\sigma_{03}\gamma_5)$, which are repulsive in the NJL model, become attractive at asymptotic density when the gluon propagator provides a form factor that strongly emphasizes small-angle scattering [28].

(4) One color and one flavor $(\mathbf{6}_S,\mathbf{3}_S,\ldots)$. There is an attractive channel here, the $(\mathbf{6}_S,\mathbf{3}_S,0,+)(C\gamma_0\gamma_5)$. It loses its particle-particle component as the quark mass goes to zero, making it very weak for up and down quarks, but quite strong for strange quarks (Fig. 4). It is suitable for the blue strange quarks in 2SC+s when red and green strange quarks have paired in the $(\bar{\mathbf{3}}_A,\mathbf{3}_S,1,+)(C\gamma_3)$ channel.

Many of the attractive channels have repulsive partners with the same symmetries, so a condensate in the attractive channel will automatically generate a small additional one in the repulsive channel. For example, the $(\bar{\mathbf{3}}_A,\mathbf{1}_A,0,+)(C\gamma_5)$ can generate $(\bar{\mathbf{3}}_A,\mathbf{1}_A,0,+)(C\gamma_0\gamma_5)$. This was discussed in Ref. [34], where the induced $(C\gamma_0\gamma_5)$ condensate (there called "κ") in 2+1 flavor CFL was calculated and found to be small. In Ref. [35] it was observed that if all three quarks are massive then this condensate may be important. In the context of CFL the $(\bar{\mathbf{3}}_A,\mathbf{1}_A,0,+)(C\gamma_5)$ can also generate $(\mathbf{6}_S,\mathbf{3}_S,0,+)(C\gamma_5)$ [7,36], since they both break the full symmetry group down to the same subgroup.

III. GAP CALCULATIONS FOR THE ATTRACTIVE DIQUARK CHANNELS

For the attractive channels we performed uncoupled gap equation calculations, and obtained the dependence of the quark pairing on μ. The amount of pairing is given by the gap parameter $\Delta(\mu)$, which occurs in the self energy (see Appendix A) as

$$\Delta_{ij}^{\alpha\beta ab}(p) = \Delta(\mu)\mathcal{C}^{\alpha\beta}\mathcal{F}_{ij}\Gamma^{ab}, \tag{3.1}$$

with color matrix $\mathcal{C}$, flavor matrix $\mathcal{F}$, and Dirac structure Γ^{ab}. Note that $\Delta(\mu)$ is a gap *parameter*, not the gap. It sets the scale of the gap in the quasiparticle excitation spectrum, but as we will see in Sec. IV the gap itself often depends on the direction of the momentum.

The four-fermion interactions that we use are nonrenormalizable, so our gap equation involves a three-momentum cutoff Λ, which represents the decoupling of our interactions at higher momentum, due to instanton form factors, effective gluon masses, etc. The usual procedure for NJL model calculations is to calibrate the coupling strength for each cutoff Λ by known low-density physics such as the size of the chiral condensate. However, it is well known that this leads to an approximately cutoff-independent maximum gap (as a function of μ) in the $\psi C\gamma_5\psi$ channel, so we used that criterion directly as our calibration condition, setting the maximum gap to 100 MeV.

The results of our calculations, for cutoff $\Lambda = 800$ MeV, are plotted in Figs. 2–4. For other cutoffs the overall shape of the curves is very similar. Because we use a sharp cutoff Λ, the gap falls to zero when μ reaches Λ [see, e.g., Eq. (A16)]. We show gap plots for the instanton interaction (Fig. 3) and magnetic gluon interaction. The full electric+magnetic gluon gives results that are similar to those for the magnetic gluon, but with no gap in the $(\mathbf{6}_S,\mathbf{1}_A,1,+)(C\sigma_{03})$ channel.

For the magnetic gluon, we show a gap plot for massless quarks (Fig. 2) which includes the two-flavor channels $(\bar{\mathbf{3}}_A,\mathbf{1}_A,0,+)(C\gamma_5)$, $(\bar{\mathbf{3}}_A,\mathbf{1}_A,1,-)(C\gamma_3\gamma_5)$, and $(\mathbf{6}_S,\mathbf{1}_A,1,+)(C\sigma_{03})$ which could sustain u-d pairing, as well as the single flavor channel $(\bar{\mathbf{3}}_A,\mathbf{3}_S,1,+)(C\gamma_3)$ which could sustain u-u or d-d pairing.

We also show a gap plot (Fig. 4) for a single quark flavor with mass of 250 or 350 MeV. This is appropriate for the strange quark, whose effective mass is expected to lie between 150 and about 400 MeV (see Ref. [12], Fig. 1).

The relative sizes of the gaps in the different channels reflect the pairing strengths given in Table I. We see that the Lorentz scalar $(\bar{\mathbf{3}}_A,\mathbf{1}_A,0,+)(C\gamma_5)$ (solid line) is dominant. The $j=1$ channels have much smaller gap parameters. The $(\bar{\mathbf{3}}_A,\mathbf{3}_S,1,+)(C\gamma_3)$ gap parameter (dash-dotted line in Figs. 2 and 4) rises to a few MeV with the magnetic gluon interaction. The $(\mathbf{6}_S,\mathbf{1}_A,1,+)(C\sigma_{03})$ gap parameter (dashed line) rises to about 1 MeV with an instanton interaction, but only 1 eV with the magnetic gluon interaction. It should be remembered, however, that the temperature of a compact star can be anything from tens of MeV at the time of the supernova to a few eV after millions of years, so gaps anywhere in this range are of potential phenomenological interest.

The $(\mathbf{6}_S,\mathbf{3}_S,0,+)(C\gamma_0\gamma_5)$ channel (dotted line), which is the only attractive channel for a single color and flavor of quark, is highly suppressed for massless quarks at high den-

sity but reaches about 10 keV for strange quarks ($m = 350$ MeV, Fig. 4). This is because its particle-particle component goes to zero as $m \to 0$ [Eq. (C9) and Table I].

Up to this point we have not mentioned the $j=1$, $m_j = \pm 1$ channels [e.g., $\psi C \gamma_\pm \psi \equiv \psi C(\gamma_1 \pm i\gamma_2)\psi$]. We have only discussed the $j=1$, $m_j=0$ channels (e.g., $\psi C \gamma_3 \psi$). That is because rotational invariance of the interaction Hamiltonian that we are using guarantees that changing m_j from 0 to ± 1 will not affect the binding energy and gap equation. This can be seen by considering the form of the binding energy. From Eq. (2.1) it is

$$E_B \sim \langle \psi\psi \rangle^{\dagger ac} \langle \psi\psi \rangle^{bd} \mathcal{H}_{abcd}. \tag{3.2}$$

Note that it is quadratic in the diquark condensate, with one of the factors being complex conjugated. So, if we have some three-vector condensate, for example $\phi = \Sigma_i \phi_i \langle \psi \gamma_i \psi \rangle$, then its binding energy is

$$E_B \propto |\phi_x|^2 + |\phi_y|^2 + |\phi_z|^2. \tag{3.3}$$

It is clear that the $m_j=0$ condensate $\phi_i = (0,0,1)$ has the same binding energy as the $m_j = \pm 1$ condensate $\phi_i = (1/\sqrt{2})(1, \pm i, 0)$. We have explicitly solved the gap equations for the $m_j = \pm 1$ condensates, and find their solutions identical to the corresponding $m_j = 0$ condensates. However, the quasiquark excitations in the two cases are quite different, and we proceed to study these in the next section.

IV. QUASIQUARK DISPERSION RELATIONS

The physical behavior of quark matter will be dominated by its lowest-energy excitations. As well as Golstone bosons that arise from spontaneous breaking of global symmetries, there will be fermionic excitations of the quarks around the Fermi surface. In the presence of a diquark condensate, the spectrum of quark excitations is radically altered. Instead of arbitrarily low-energy degrees of freedom, associated with the promotion of a quark from a state just below the Fermi surface to just above it, there is a minimum excitation energy (gap), above which the excitation spectrum is that of free quasiquarks, which are linear combinations of a particle and a hole.

The dispersion relations of the quasiparticles can be calculated straightforwardly by including a condensate of the desired structure in the inverse propagator S^{-1}, shown in Eq. (A3). Poles in the propagator correspond to zeros in S^{-1}, so the dispersion relations are obtained by solving $\det S^{-1}(p_0, \mathbf{p}, \mu, \Delta, m) = 0$ for the energy p_0 as a function of the three-momentum $\mathbf{p}$ of the quasiparticle, quark chemical potential μ, gap parameter Δ, and quark mass m.

The gap is by definition the energy required to excite the lowest-energy quasiquark mode. Isotropic condensates have a uniform gap, but one of the most interesting features of $j>0$ condensates is that they are not in general fully gapped: the gap goes to zero for particular values of momentum $\mathbf{p}$, which correspond to particular places on the Fermi surface. This means that transport properties such as viscosities and emissivities, which are suppressed by factors of $\exp(-\Delta/T)$ in phases with isotropic quark pairing, may not be so strongly suppressed by a $j>0$ condensate. In Figs. 5 and 6 we show the variation of the gap over the Fermi surface by plotting the energy of the lowest excitation as a function of angle,

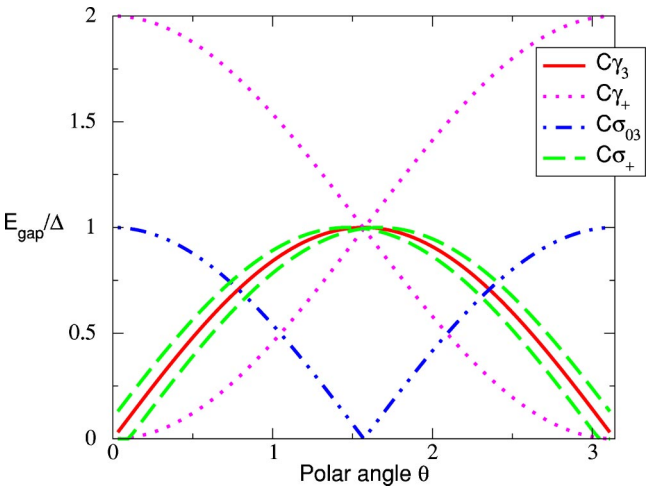

FIG. 5. Energy gap in units of the gap parameter as a function of polar angle on the Fermi surface for rotational symmetry breaking phases with massless quarks, at $\mu = 500$ MeV, gap parameter $\Delta = 50$ MeV, $\gamma_+ \equiv \gamma_1 + i\gamma_2$, $\sigma_+ \equiv \sigma_{01} + i\sigma_{02}$.

$$E_{\rm gap}(\theta) = \min_{p,i} |E_i(p,\theta)|, \tag{4.1}$$

where $E_i(p,\theta)$ is the energy of the ith quasiquark excitation with momentum $(p \sin\theta\cos\phi, p\sin\theta\sin\phi, p\cos\theta)$. For the plots we take $\mu = 500$ MeV and $\Delta = 50$ MeV, with quark mass $m=0$ (Fig. 5) or $m = 250$ MeV (Fig. 6).

(1) $C\gamma_3$ condensate: $j=1$, $m_j=0$. There is one quasiquark excitation with energy less than the gap parameter Δ:

$$E(p)^2 = (\sqrt{p^2 + m^2\mu^2/\mu_{\rm eff}^2} \pm \mu_{\rm eff})^2 + \Delta_{\rm eff}^2,$$

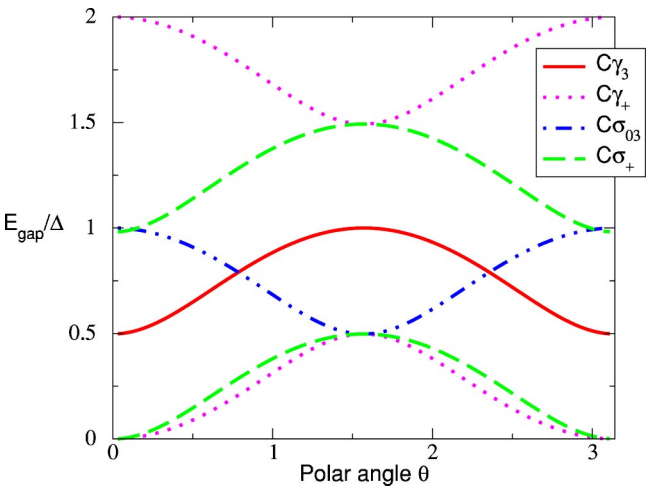

FIG. 6. Energy gap in units of the gap parameter as a function of polar angle on the Fermi surface for rotational symmetry breaking phases at $\mu = 500$ MeV, with gap parameter $\Delta = 50$ MeV. The quarks have mass $m = 250$ MeV, $\gamma_+ \equiv \gamma_1 + i\gamma_2$, $\sigma_+ \equiv \sigma_{01} + i\sigma_{02}$.

$$\mu_{\rm eff}(\theta)^2=\mu^2+\Delta^2\cos^2(\theta),$$
$$\Delta_{\rm eff}(\theta)^2=\Delta^2[\sin^2(\theta)+m^2/\mu_{\rm eff}^2\cos^2(\theta)]. \quad (4.2)$$

From the expression for $\Delta_{\rm eff}(\theta)$ we see that for massless quarks the gap goes to zero for momenta parallel to the z axis, i.e., at the poles on the Fermi surface (solid curve in Fig. 5). Massive quarks retain a small gap of order $m\Delta/\mu$ at the poles (solid curve in Fig. 6).

(2) $C(\gamma_1\pm i\gamma_2)$ condensate: $j=1$, $m_j=\pm1$. There are two quasiquark excitations with energy less than 2Δ,

$$E(p)^2=2\Delta^2+m^2+\mu^2+p^2\pm\{4\Delta^4+4\mu^2(p^2+m^2)+2\Delta^2p^2[1-\cos(2\theta)]\pm4\Delta^2\mu\sqrt{4m^2+2p^2[1+\cos(2\theta)]}\}^{1/2}. \quad (4.3)$$

For this condensate the effective gap again goes to zero at the poles, but in this case it remains zero even in the presence of a quark mass (dotted curve in Figs. 5 and 6).

(3) $C\sigma_{03}$ condensate: $j=1$, $m_j=0$. There is one quasiquark excitation with energy less than Δ; its dispersion relation is [29]

$$E(p)^2=(\sqrt{p^2+m^2\mu^2/\mu_{\rm eff}^2}\pm\mu_{\rm eff})^2+\Delta_{\rm eff}^2,$$
$$\mu_{\rm eff}(\theta)^2=\mu^2+\Delta^2\sin^2(\theta),$$
$$\Delta_{\rm eff}(\theta)^2=\Delta^2[\cos^2(\theta)+m^2/\mu_{\rm eff}^2\sin^2(\theta)]. \quad (4.4)$$

This is related to the dispersion relation for the $C\gamma_3$ condensate by $\theta\to\pi/2-\theta$: for massless quarks the quasiquarks are gapless around the equator of the Fermi sphere (dash-double-dotted curve in Fig. 5) and in the presence of a quark mass they gain a small gap of order $\Delta m/\mu$ (dash-double-dotted curve in Fig. 6). The equator is a larger proportion of the Fermi surface than the poles, so in this case we might expect a greater effect on transport properties.

(4) $C(\sigma_{01}\pm i\sigma_{02})$ condensate: $j=1$, $m_j=\pm1$. There are two quasiquark excitations with energy less than Δ. They have rather complicated dispersion relations. Going to the massless case, and assuming $E,(p-\mu)\ll\mu$, which will be true for the low-energy quasiquark degrees of freedom that we are interested in, we find

$$E_{(p)}=[\Delta^2\mu+\Delta^2p\cos(\theta)\pm\eta/\sqrt{2}]/(2\mu^2),$$
$$\eta^2=\{8\mu^4(\mu-p)^2+8\Delta^2\mu^2[\mu^2-\cos(\theta)^2p^2]+2\Delta^4[\mu+\cos(gv)p]^2\}. \quad (4.5)$$

In this case there is a region near the poles, $\theta\lesssim\Delta/\mu$, where the gap is zero (dashed curve in Fig. 5). This is because at those angles $E(p)$ has zeros at two values of p close to μ. When $\theta\approx\Delta/\mu$ those two zeros merge and disappear from the real p axis. The presence of a quark mass $m>\Delta$ wipes out this effect, but there is still no gap at the poles on the Fermi surface (dashed curve in Fig. 6).

In comparing Figs. 5 and 6 it is interesting to note that introducing a mass for the quark opens up a gap whenever the gap lines intersect each other at a nonzero angle (after one includes the mirror-image negative-energy gap curves for the quasiholes). This occurs at zero energy at the poles for $C\gamma_3$ and at the equator for $C\sigma_{03}$. It occurs at nonzero energy for $C(\gamma_1\pm i\gamma_2)$. The case of $C(\sigma_{01}\pm i\sigma_{02})$ is similar, but it is not obvious from the gap plot for reasons described above.

We see that the $j\neq0$ phases show a rich variety of quasiquark dispersion relations. For massless quarks they are all gapless in special regions of the Fermi surface, and for massive quarks the $m_j=\pm1$ condensates remain gapless for momenta parallel to the spin. It follows that for these phases the quasiquark excitations will play an important role in transport properties, even when the temperature is less than the gap parameter.

Moreover, different condensates ($m_j=\pm1$ vs $m_j=0$), which because of rotational invariance of the Hamiltonian have exactly the same binding energy and gap equation, nevertheless have completely different energy gaps over the Fermi surface. They will therefore behave quite differently when exposed to nonisotropic external influences, such as magnetic fields or neutrino fluxes, and also in their coupling to external sources of torque, e.g., via electron-quasiquark scattering. All these influences are present in compact stars, and it will be interesting and complicated to sort out which is favored under naturally occurring conditions. And it should not be forgotten that these conditions vary with the age of the star.

V. MESONIC CONDENSATES

Berges and Wetterich [30] have invoked ideas of complementarity to suggest that the confining QCD vacuum could be understood in terms of non-color-singlet chiral condensates. We can study the attractiveness of such channels by mean-field methods similar to those of Sec. II.

A mesonic condensate X with strength $A_{(X)}$ is

$$\langle\overline{\psi}^i_{\alpha a}\psi^{\beta b}_j\rangle=A_{(X)}\mathfrak{CF}_{(X)}{}^{\beta i}_{\alpha j}\Gamma_{(X)}{}^b_a \quad (5.1)$$

where $\mathfrak{CF}$ is the color-flavor structure of the mesonic condensate. We can calculate their binding energy by contracting them with Eq. (2.2), and the energy is given by Eq. (2.4), where as before the binding strengths $S^{(X)}_{\rm interaction}$ give the strength of the self-interaction of the condensate X due to the specified part of the interaction Hamiltonian. Unlike the diquark condensates, there are two possible contractions, the Hartree contribution and the Fock contribution, since there are two possible $\psi^\dagger$ to contract with each ψ. Again there is no Fierz ambiguity, and we include both Hartree and Fock contributions.

For consistency we have used the same three interactions, namely, instanton, full (electric plus magnetic) gluon, and magnetic gluon, as in our treatment of quark pairing. However, it should be noted that the main relevance of quark-antiquark pairing is at low density, where there is no reason to expect the magnetic gluon to predominate, so in the case of Table II the final column does not have any special physical relevance.

TABLE II. Quark-antiquark pairing strength in various rotationally symmetric channels.

Structure of condensate		Attractiveness		
Color-flavor	Dirac	Instanton	Magnetic+electric gluon	Magnetic gluon
(**1**,**1**)	1	+192	+192	+144
(**1**,**1**)	γ_5	−192	+192	+144
(**1**,**1**)	γ_0	0	−96	−144
(**1**,**1**)	$i\gamma_0\gamma_5$	0	−96	−144
(**8**,**8**)	1	−6	−12	−9
(**8**,**8**)	γ_5	+6	−12	−9
(**8**,**8**)	γ_0	0	+6	+9
(**8**,**8**)	$i\gamma_0\gamma_5$	0	+6	+9
(**8**,**1**)	1	+24	−48	−36
(**8**,**1**)	γ_5	−24	−48	−36
(**8**,**1**)	γ_0	0	−300	+36
(**8**,**1**)	$i\gamma_0\gamma_5$	0	−12	+36

The color-flavor structures that we study are

$$\mathfrak{CF}_{(\mathbf{8},\mathbf{8})^{\alpha j}_{\beta i}} = \delta^\beta_j \delta^i_\alpha - \tfrac{1}{2}\delta^\beta_\alpha \delta^i_j,$$

$$\mathfrak{CF}_{(\mathbf{1},\mathbf{1})^{\alpha j}_{\beta i}} = \delta^i_j \delta^\beta_\alpha, \tag{5.2}$$

$$\mathfrak{CF}_{(\mathbf{8},\mathbf{1})^{\alpha j}_{\beta i}} = \delta^i_j (\delta^\beta_\alpha \delta^\beta_1 + \delta^\beta_\alpha \delta^\beta_2 - 2\delta^\beta_\alpha \delta^\beta_3).$$

The (**1**,**1**) is a singlet in color and flavor. The (**8**,**8**) is a color-flavor-locked adjoint chiral condensate, of the kind posited in Ref. [30]. We have studied it in the two-flavor case, where the two flavors lock to two of the three colors (red and green, say). The (**8**,**1**) is a flavor-singlet condensate with color structure (1,1,−2), so it spontaneously selects a color direction that we have fixed as blue.

The Dirac structures are two chiral condensates 1 and γ_5 (scalar and pseudoscalar, respectively), and two that contain a γ_0 and therefore correspond to a number density of quarks. N_R+N_L for γ_0, i.e., a renormalization of the chemical potential, and N_R-N_L for $\gamma_0\gamma_5$.

The results are given in Table II. We see that the standard chiral condensate (**1**,**1**)(1) is overwhelmingly favored over all the others. Its pseudoscalar partner $(\mathbf{1},\mathbf{1})(\gamma_5)$ is disfavored by instantons.

Among the color-flavor-locked adjoint condensates, the interaction energies are much weaker. The Lorentz scalar (**8**,**8**)(1) studied in Ref. [30] is disfavored by all the interactions, but its pseudoscalar partner $(\mathbf{8},\mathbf{8})(\gamma_5)$ is less disfavored, thanks to a positive contribution from instantons. Interestingly, the only favored adjoint condensates are the ones that correspond to spontaneous generation of particle number, the $(\mathbf{8},\mathbf{8})(\gamma_0)$ and its pseudoscalar partner.

The color-adjoint flavor-singlet condensates show larger interaction energies than the color-flavor-locked adjoint condensates, but mostly they are repulsive. The very large repulsion for the $(\mathbf{8},\mathbf{1})(\gamma_0)$ in the electric gluon channel comes from the Hartree term, and corresponds to the enormous Coulomb repulsion of a spontaneously generated uniform density of blue quarks. This color imbalance does not arise in other condensates: in the color-flavor-locked $(\mathbf{8},\mathbf{8})(\gamma_0)$ each flavor favors a different color, and in the $(\mathbf{8},\mathbf{8})(i\gamma_0\gamma_5)$ the left-handed and right-handed quarks have opposite color. If instantons predominate then the (**8**,**1**)(1) condensate would be the strongest competitor to the standard chiral condensate.

VI. SUMMARY

As we discussed in the Introduction, it currently seems plausible that there are three general types of neutral quark matter that may be found in the mysterious non-color-flavor-locked wedge in the high strange quark mass and high density region of the m_s-μ plane (Fig. 1). These are single flavor pairing only (1SC), two-flavor pairing of *u* and *d* quarks with additional single flavor pairing of the remaining species (2SC+1SC), and three-flavor crystalline (LOFF) pairing.

The competition between these is influenced by the strange quark mass, which increases the energy cost of *s* quarks, depressing their Fermi momentum; the requirement of electrical neutrality, which increases the number of *u* quarks to compensate for the smaller number of *s* quarks; and the energy gain that quarks obtain by pairing.

In this paper, we have investigated some of the specific pairing patterns that are found under these general categories, paying particular attention to single flavor and single color pairing channels. We have studied the factorizable (nonlocked) color-flavor-spin quark pairing condensates that occur in a NJL model of QCD that uses pointlike four-fermion interactions (Table I). Our survey includes all the allowed color and flavor structures, and those spin structures that can be formed from two quark fields and a general Dirac matrix. We did not include higher angular momenta introduced by explicit spatial derivatives, nor spatially inhomogeneous condensates in our calculations. We have solved the gap equation for the attractive channels, and obtained the relative sizes of their gap parameters (Figs. 2–4).

Our conclusions are as follows.

(1) Single-flavor pairing (1SC). If the strange quark mass is large enough then charge neutrality requirements will force all three flavors to have Fermi momenta too far apart to allow any BCS pairing of different flavors. In this case, each flavor will have to self-pair (Fig. 7).[1] Our calculations indicate that two colors (red and green, say) can pair via gluon interactions in the $(\overline{\mathbf{3}}_A,\mathbf{3}_S,1,+)(C\gamma_3)$ channel, and the blue *s* quarks can then pair in the rotationally invariant $(\mathbf{6}_S,\mathbf{3}_S,0,+)(C\gamma_0\gamma_5)$. Note that these pairing patterns, being flavor symmetric, only exist for the single gluon interaction,

[1]For a strange quark mass that is large (probably unphysically so), there will be a region in the quark matter part of the m_s-μ plane where $\mu<m_s$, so there are no *s* quarks and the *u* and *d* Fermi momenta differ by some appreciable fraction of μ. This region is described by Fig. 7 or Fig. 8 but with the strange quark Fermi momentum set to zero, so no pairing of strange quarks.

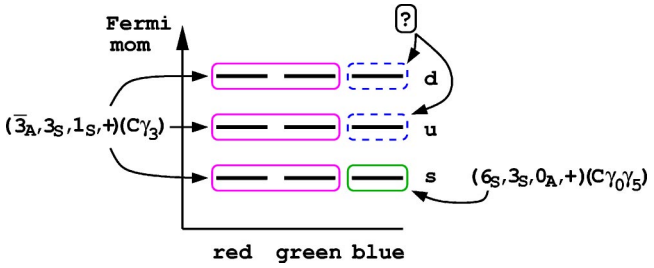

FIG. 7. Pictorial representation of single flavor pairing (1SC) in neutral quark matter. The requirement of electric neutrality and a nonzero strange quark mass forces the Fermi momenta of the three flavors apart. The red and green colors of each flavor pair in a color-antisymmetric channel. The blue *s* quark self-pairs in a color- and flavor-symmetric channel. We have not found an attractive channel in which the blue *u* or blue *d* could pair. Competing pairing patterns for the same arrangement of Fermi momenta are color-spin locking and the CFL-LOFF phase (see text).

not the instanton interaction. This makes them more model dependent than the $(\bar{\mathbf{3}}_A,\mathbf{1}_A,0,+)(C\gamma_5)$, whose strength is approximately independent of the interaction used.

This leaves the blue *u* quarks and *d* quarks. We have not found a single color and single flavor channel that can pair massless quarks, so they will have to find an attractive channel outside the set that we have explored here. An alternative possibility is that for each flavor there is color-spin-locked condensation of all three colors.

(2) Two-flavor *u*-*d* and additional single flavor pairing (2SC+1SC). It is just possible that there is a range of m_s in which 2SC *u*-*d* pairing can occur. m_s must be high enough so that CFL or CFL-K^0 is disfavored relative to 2SC, but low enough so that the *u* and *d* Fermi momenta are close enough to allow them to pair with each other. The energy accounting is complicated by contributions from the chiral condensate, which competes more or less strongly with different quark pairing patterns. Current indications are that 2SC either does not occur, or survives only in a very narrow window [19,20]. The pairings involved in 2SC+1SC are depicted in Fig. 8. The red and green *u* and *d* quarks undergo 2SC pairing. The blue quarks and the strange quarks follow the same pairing patterns as in the single flavor pairing case. Note that enforcing color neutrality will create a small $\mathcal{O}(\Delta^2/\mu)$ splitting between the Fermi momentum of the blue *s* and that of the red and green *s*. This may prevent color-spin locking for the *s* quarks.

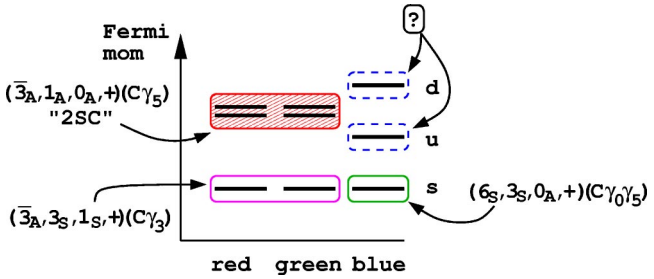

FIG. 8. Pictorial representation of 2SC+*s* with additional single-flavor pairing in neutral quark matter. This will only occur if the condensation energy of the 2SC pairing is strong enough to offset the cost of dragging the red and green *u* and *d* Fermi momenta away from the values dictated by electric neutrality and the strange quark mass, to a common value.

(3) Three-flavor crystalline pairing (LOFF). An important competitor to the channels discussed here is the LOFF phase, in which flavors that cannot undergo conventional BCS pairing because their Fermi momenta are too far apart can nevertheless pair over part of their Fermi surfaces by forming pairs with net momentum. This breaks translational invariance, and leads to a crystal structure [25,26]. One can imagine a type of CFL-LOFF pairing, in which the red and green *u* and *d* quarks, the red and blue *u* and *s* quarks, and the blue and green *d* and *s* quarks all form LOFF pairs. A recent Ginzburg-Landau study [27] indicates that the condensation energy of the crystalline phase may be large enough to beat any single flavor channel, although this result followed from extrapolating the Ginzburg-Landau analysis beyond its realm of validity.

As well as evaluating the attractiveness of a large set of channels, we have calculated the angular dependence over the Fermi surface of the energies of the quasiquark excitations associated with each of the $j=1$ quark pair condensates. We see that the $j=1$, $m_j=\pm 1$ condensates always have gapless quasiquarks at the poles of the Fermi sphere. The $j=1$, $m_j=0$ condensates have gapless regions for massless quarks, at the poles $(\psi C\gamma_3\psi)$ or around the equator $(\psi C\sigma_{03}\psi)$, but if the quarks are massive then the quasiquarks have a minimum gap of order $m\Delta/\mu$ (Figs. 5 and 6). The gapless points or lines on the Fermi surface are likely to lead to interesting phenomenology (see below).

Finally, we have surveyed the isotropic mesonic condensates, and find that the conventional chiral condensate is very heavily favored. The color-flavor-locked mesonic channel studied in Ref. [30] is strongly disfavored, as was noted in Ref. [37]. It has been argued [38] that taking into account the effect of the color-flavor-locked channel on the integral over instanton sizes makes the condensation energy come out attractive after all.

VII. THE ROAD AHEAD

This work can be extended in many directions, and points to interesting questions in the theory of dense matter and compact star phenomenology.

A. Dense matter

(1) In order to allow comparisons between the phases we studied and other competing possibilities such as the LOFF phase, it would be useful to calculate the free energy of the various 1SC pairing patterns. (2) It would be valuable to extend our survey to include an even wider set of possible quark pair condensation patterns, such as color-spin locking. We would also like to find a channel in which light single color single flavor pairing can occur. It might be necessary to explore condensates where orbital angular momentum is introduced explicitly via derivatives, $\psi C\partial_\mu\psi$, etc. These momentum-dependent condensates will not arise from the

mean-field treatment of the simplified pointlike interactions that we used. One would have to give the four-fermion vertex a nontrivial form factor, or go beyond the mean-field approximation. (3) A related area that is already being investigated is single color/flavor channels in the ultrahigh-density region with the true QCD interaction vertex, including the hard dense loop resummed gluon propagator [28,16,33]. In this regime one will also find momentum-dependent gaps. (4) We studied the attractive channels independently of each other, and independent of chiral condensation. It is clearly necessary to solve their coupled gap equations, and see how they compete or coexist. (5) We only worked at zero temperature. It is straightforward to generalize the gap equations to arbitrary temperature, and recent work indicates that the usual BCS relationship between the critical temperature and the gap parameter may be modified for these exotic condensates [29,33].

B. Compact star phenomenology

Although many of the channels we studied have very small gaps and therefore very small critical temperatures, they will be phenomenologically relevant if they are the best pairing option available for some of the quarks. Since the temperature of a compact star falls to tens of eV when its age reaches about a million years, pairing can suddenly occur in such channels late in the star's life, and the corresponding quasiquark excitations will suddenly become too heavy to participate in transport processes. We must remember, however, that some of the exotic channels are gapless at special three-momenta. In those cases a small proportion of their quasiparticles may continue to play a role in transport properties, even when the temperature is much less than the gap parameter. Some specific topics for further investigation are as follows: (1) Develop the transport theory of $j\neq 0$ condensates: they have gapless modes at points or along lines on their Fermi surface. What effect does this have on neutrino emission or absorption via URCA processes or otherwise, their specific heat, viscosities, conductivities, etc.? A natural first step would be to write down an effective theory, which would contain the lowest quasiquark modes, Goldstone bosons arising from the breaking of rotational symmetry (which could be called ''spin waves'' by analogy with ^{3}He), and density waves. (2) The $j=1$ condensates can carry angular momentum simply by aligning themselves in large domains, without involving any superfluid vortices, but it seems they will typically occur in conjunction with other phases that are superfluid. It would be interesting to see how the angular momentum is carried in this situation. (3) The $j=1$ condensates are ferromagnets. It would be interesting to see if they could generate large magnetic fields such as those suggested for magnetars (10^{14}–10^{15} G). (4) The various $j=1$ condensates show completely different variation of the energy gap over the Fermi surface (Sec. IV). It would be useful to know how they behave when exposed to the nonisotropic external influences that are common in compact stars, such as magnetic fields or neutrino fluxes, and also in their coupling to external sources of torque, e.g., via electron-quasiquark scattering.

Clearly there remain many interesting questions, both formal and phenomenological, about the single color and/or single flavor-color superconducting phases of dense quark matter.

ACKNOWLEDGMENTS

The work of M.G.A. and G.A.C. is supported by the U.K. PPARC. The work of J.A.B. is supported by the U.S. Department of Energy (DOE) under cooperative research agreement no. DF-FC02-94ER40818 and by the DOD National Defense Science and Engineering Graduate program. The work of J.M.C. is supported by funding from Glasgow University and the Glasgow University physics department. M.G.A. and J.A.B. acknowledge the Kavli Institute for Theoretical Physics for providing a stimulating venue for part of this work. We thank Krishna Rajagopal for very valuable discussions, and Thomas Schäfer for comments on an earlier draft.

APPENDIX A: CALCULATIONAL DETAILS

To allow the possibility of quark pairing, we use eight-component Nambu-Gorkov spinors:

$$\Psi=\begin{pmatrix}\psi(p)\\ \bar{\psi}^T(-p)\end{pmatrix} \tag{A1}$$

with

$$\bar{\Psi}=(\bar{\psi}(p),\psi^T(-p)). \tag{A2}$$

In Minkowski space the inverse quark propagator for massive fermions takes the form

$$S^{-1}(p)=\begin{pmatrix}\not{p}-m+\mu\gamma_0 & \bar{\Delta}\\ \Delta & (\not{p}+m-\mu\gamma_0)^T\end{pmatrix} \tag{A3}$$

where

$$\bar{\Delta}=\gamma_0\Delta^\dagger\gamma_0. \tag{A4}$$

The gap matrix Δ is a matrix in color, flavor, and Dirac space, multiplied by a gap parameter also denoted as Δ:

$$\Delta_{ij}^{\alpha\beta ab}=\Delta(\mu)C^{\alpha\beta}\mathcal{F}_{ij}\Gamma^{ab}. \tag{A5}$$

The relation between the proper self-energy and the full propagator is

$$S^{-1}=S_0^{-1}+\Sigma=\begin{pmatrix}\not{p}-m+\mu\gamma_0 & 0\\ 0 & (\not{p}+m-\mu\gamma_0)^T\end{pmatrix}+\begin{pmatrix}0 & \bar{\Delta}\\ \Delta & 0\end{pmatrix} \tag{A6}$$

where S_0^{-1} is the inverse propagator in the absence of interactions. The gap is determined by solving a self-consistent Schwinger-Dyson equation for Σ. For a four-fermion interaction modeling single gluon exchange, this takes the form

$$\Sigma = -6iG \int \frac{d^4p}{(2\pi)^4} V_\mu^A S(p) V^{A\mu} \tag{A7}$$

where V_μ^A is the interaction vertex in the Nambu-Gorkov basis. We study three interactions, the quark-gluon vertex

$$V_\mu^A = \begin{pmatrix} \gamma_\mu \lambda^A/2 & 0 \\ 0 & -(\gamma_\mu \lambda^A/2)^T \end{pmatrix}, \tag{A8}$$

the quark-magnetic gluon vertex

$$V_i^A = \begin{pmatrix} \gamma_i \lambda^A/2 & 0 \\ 0 & -(\gamma_i \lambda^A/2)^T \end{pmatrix}, \tag{A9}$$

and the quark-instanton vertex, for which

$$\Sigma_{ik}^{\alpha\gamma} = -6iG \int \frac{d^4p}{(2\pi)^4} [V_{L\mu}^A S_{jl}^{\beta\delta}(p) V_L^{A\mu} + V_{R\mu}^A S_{jl}^{\beta\delta}(p) V_R^{A\mu}] \Xi_{ik\beta\delta}^{jl\alpha\gamma} \tag{A10}$$

where

$$\Xi_{ik\beta\delta}^{jl\alpha\gamma} = -\varepsilon_{ik}\varepsilon^{jl}\frac{2}{3}(3\delta_\beta^\alpha\delta_\delta^\gamma - \delta_\delta^\alpha\delta_\beta^\gamma) \tag{A11}$$

and

$$V_L^A = \begin{pmatrix} (\mathbf{1}+\gamma_5) & 0 \\ 0 & (\mathbf{1}+\gamma_5)^T \end{pmatrix}$$

and

$$V_R^A = \begin{pmatrix} (\mathbf{1}-\gamma_5) & 0 \\ 0 & (\mathbf{1}-\gamma_5)^T \end{pmatrix}. \tag{A12}$$

In the case of the $\psi C\gamma_5\psi$ condensate for the full gluon interaction we obtain the gap equation, which after rotation to Euclidean space becomes

$$1 = 16G \int \frac{dp_0 d^3p}{(2\pi)^4} \frac{4(\Delta^2+\mu^2+p_0^2+p^2)}{W} \tag{A13}$$

where

$$W = \Delta^4 + \mu^4 + (p_0^2+p^2)^2 + 2\Delta^2(\mu^2+p_0^2+p^2) - 2\mu^2(-p_0^2+p^2). \tag{A14}$$

The p_0 integral can be explicitly evaluated,

$$1 = \frac{2G}{\pi^2}\int_0^\Lambda dp \left[\frac{p^2}{\sqrt{\Delta^2+(p+\mu)^2}} + \frac{p^2}{\sqrt{\Delta^2+(p-\mu)^2}} \right]. \tag{A15}$$

The momentum integral can be performed analytically, giving

$$\Delta = 2\sqrt{\Lambda^2-\mu^2}\exp\left(\frac{\Lambda^2-3\mu^2}{2\mu^2}\right)\exp\left(-\frac{\pi^2}{4\pi^2 G}\right) \tag{A16}$$

for $\Delta \ll \mu$.

APPENDIX B: GAP EQUATION SUMMARY

Here are the gap equations for the attractive channels. In the following, positive square roots are implied and we define $p_r^2 \equiv (p_x)^2 + (p_y)^2$.

$$\int d|p| \equiv \int_0^\Lambda d|p|, \quad \int dp_r dp_z \equiv \int_0^\Lambda dp_r \int_{-\sqrt{\Lambda^2-p_r^2}}^{\sqrt{\Lambda^2-p_r^2}} dp_z .$$

1. $C\gamma_5$ and C gap equations

$$1 = N\frac{G}{\pi^2}\int d|p| \left[\frac{|p|^2}{\sqrt{\Delta^2+(|p|-\mu)^2}} + \frac{|p|^2}{\sqrt{\Delta^2+(|p|+\mu)^2}} \right] \tag{B1}$$

where N is a constant that differs for each interaction:

Instanton: $N=4$,

Magnetic + electric gluon: $N=2$,

Magnetic gluon: $N=\frac{3}{2}$.

The C channel produces an identical gap equation for both the full gluon and magnetic gluon interactions. The instanton interaction is not attractive in this channel.

2. $C\sigma_{03}$ and $C\sigma_{03}\gamma_5$ gap equations

$$1 = N\frac{G}{\pi^2}\int dp_r dp_z \left[\frac{p_r(\mathcal{E}+p_r^2)}{\mathcal{E}E_+} + \frac{p_r(\mathcal{E}-p_r^2)}{\mathcal{E}E_-} \right] \tag{B2}$$

with

$$\mathcal{E}^2 = \Delta^2 p_r^2 + \mu^2|p|^2,$$

$$E_\pm^2 = \Delta^2 + \mu^2 + |p|^2 \pm 2\mathcal{E},$$

where N is a constant that differs for each interaction:

Instanton: $N=1$,

Magnetic gluon: $N=\frac{1}{8}$.

The $C\sigma_{03}\gamma_5$ channel produces an identical gap equation for magnetic gluon interaction. The instanton and the full gluon interactions are not attractive in this channel.

3. $C(\sigma_{01}\pm i\sigma_{02})$ gap equation

$$1=N\frac{-iG}{\pi^3}\int dp_r dp_z\int_{-\infty}^{\infty}dp^0 \times\frac{p_r(\mu^2-(p^0)^2-p_z^2-2p^0p_z)}{W} \tag{B3}$$

where

$$W=\mu^4+[-(p^0)^2+|p|^2]^2+2\Delta^2[\mu^2-(p^0)^2-p_z^2-2p^0p_z] -2\mu^2[(p^0)^2+|p|^2]$$

and N is a constant that differs for each interaction:

Instanton: $N=2$,

Magnetic gluon: $N=\frac{1}{4}$.

4. $C\gamma_3$ gap equation

$$1=N\frac{G}{\pi^2}\int dp_r dp_z\left[\frac{p_r(\mathcal{E}+p_z^2)}{\mathcal{E}E_+}+\frac{p_r(\mathcal{E}-p_z^2)}{\mathcal{E}E_-}\right] \tag{B4}$$

with

$$\mathcal{E}^2=\Delta^2p_z^2+\mu^2(|p|^2+m^2),$$

$$E_\pm^2=\Delta^2+\mu^2+m^2+|p|^2\pm 2\mathcal{E},$$

where N is a constant that differs for each interaction:

Magnetic+electric gluon: $N=\frac{1}{2}$,

Magnetic gluon: $N=\frac{1}{4}$.

5. $C\gamma_3\gamma_5$ gap equation

This channel is not attractive for instantons and its gap equation with electric or magnetic gluon interaction is the same as for the massless $C\gamma_3$ channel, i.e.,

$$1=N\frac{G}{\pi^2}\int dp_r dp_z\left[\frac{p_r(\mathcal{E}+p_z^2)}{\mathcal{E}E_+}+\frac{p_r(\mathcal{E}-p_z^2)}{\mathcal{E}E_-}\right] \tag{B5}$$

with

$$\mathcal{E}^2=\Delta^2p_z^2+\mu^2|p|^2,$$

$$E_\pm^2=\Delta^2+\mu^2+|p|^2\pm 2\mathcal{E},$$

where

Magnetic+electric gluon: $N=\frac{1}{2}$,

Magnetic gluon: $N=\frac{1}{4}$.

6. $C(\gamma_1\pm i\gamma_2)$ gap equation

$$1=N\frac{-iG}{\pi^3}\int dp_r dp_z\int_{-\infty}^{\infty}dp^0\frac{p_r\{2\Delta^2E_{1-}E_{1+}+[m^2+\mu^2-(p^0)^2+p_z^2]E_{2-}E_{2+}\}}{E_{1-}E_{1+}\{4\Delta^4+4\Delta^2[m^2+\mu^2-(p^0)^2+p_z^2]+E_{1-}E_{1+}\}} \tag{B6}$$

with

$$E_{1\pm}=m^2-(\mu\pm p^0)^2+p_z^2,$$

$$E_{2\pm}=m^2-(\mu\pm p^0)^2+|p|^2,$$

where N is a constant that differs for each interaction:

Magnetic+electric gluon: $N=1$,

Magnetic gluon: $N=\frac{1}{2}$.

7. $C\gamma_0\gamma_5$ gap equation

$$1=N\frac{G}{\pi^2}\int d|p|\left[\frac{|p|^2(\mathcal{E}+|p|^2)}{\mathcal{E}E_+}+\frac{|p|^2(\mathcal{E}-|p|^2)}{\mathcal{E}E_-}\right] \tag{B7}$$

with

$$\mathcal{E}^2=\Delta^2|p|^2+\mu^2(|p|^2+m^2),$$

$$E_\pm^2=\Delta^2+\mu^2+m^2+|p|^2\pm 2\mathcal{E},$$

where N is a constant that differs for each interaction:

Magnetic+electric gluon: $N=\frac{1}{2}$,

Magnetic gluon: $N=\frac{3}{4}$.

For $m=0$ this reduces to

$$1=N\frac{2G}{3\pi^2}\frac{\Lambda^3}{\sqrt{\Delta^2+\mu^2}}. \tag{B8}$$

APPENDIX C: ORBITAL AND SPIN CONTENT OF THE CONDENSATES

In the nonrelativistic limit it is meaningful to ask about the separate contributions of the orbital and spin angular momenta to the total angular momentum of the diquark condensates. We can identify these by expanding the field operators

out of which the condensates are built in terms of creation and annihilation operators,

$$\psi_i^\alpha = \sum_{k,s} \left(\frac{m}{VE_k}\right)^{1/2} [u^s(k) a^s_{ki\alpha} e^{-ikx} + v^s(k) b^{s\dagger}_{ki\alpha} e^{ikx}]. \tag{C1}$$

Inserting the explicit momentum-dependent spinors in any basis allows the creation and annihilation operator expansions of the condensates to be calculated.

In the Dirac basis,

$$u_1^D(\mathbf{k}) = A\begin{pmatrix} 1 \\ 0 \\ Bk_3 \\ B(k_1+ik_2) \end{pmatrix}, \quad u_2^D(\mathbf{k}) = A\begin{pmatrix} 0 \\ 1 \\ B(k_1-ik_2) \\ -Bk_3 \end{pmatrix}, \tag{C2}$$

$$v_1^D(\mathbf{k}) = A\begin{pmatrix} B(k_1-ik_2) \\ -Bk_3 \\ 0 \\ 1 \end{pmatrix}, \quad v_2^D(\mathbf{k}) = A\begin{pmatrix} Bk_3 \\ B(k_1+ik_2) \\ 1 \\ 0 \end{pmatrix},$$

$$A = \left(\frac{E+m}{2m}\right)^{1/2}, \quad B = \frac{1}{E+m}. \tag{C3}$$

Equation (C4) shows the result of performing such a calculation for the $\psi C\psi$ condensate,

$$\begin{aligned} \psi C\mathcal{S}\psi = \frac{1}{E}[&(a^2_{pi\alpha}a^2_{-pj\beta} + b^{\dagger 1}_{pi\alpha}b^{\dagger 1}_{-pj\beta})(p_1 - ip_2) \\ &- (a^1_{pi\alpha}a^1_{-pj\beta} + b^{\dagger 2}_{pi\alpha}b^{\dagger 2}_{-pj\beta})(p_1 + ip_2) \\ &+ 2(a^1_{pi\alpha}a^2_{-pj\beta} + b^{\dagger 1}_{pi\alpha}b^{\dagger 2}_{-pj\beta})p_3]\mathcal{S}^{ij}_{\alpha\beta}, \end{aligned} \tag{C4}$$

where $\mathcal{S}^{ij}_{\alpha\beta}$ is the color-flavor matrix which is symmetric under the interchange $i \rightleftharpoons j$ (flavor) and $\alpha \rightleftharpoons \beta$ (color). A sum over momentum p should be performed on the right-hand side.

Once the operator expansions have been obtained it is a relatively simple procedure to obtain the angular momentum content by rearranging the terms and inserting the relevant spherical harmonics. It is important to include contributions from momenta k and $-k$ together, since they involve the same creation and annihilation operators. For example, for the condensate in Eq. (C4),

$$\begin{aligned} p = k\text{:}\ \frac{1}{E}[&a^2_{ki\alpha}a^2_{-kj\beta}(k_1 - ik_2) - a^1_{ki\alpha}a^1_{-kj\beta}(k_1 + ik_2) \\ &+ 2a^1_{ki\alpha}a^2_{-kj\beta}k_3], \end{aligned} \tag{C5}$$

$$\begin{aligned} p = -k\text{:}\ &\frac{1}{E}[-a^2_{-ki\alpha}a^2_{kj\beta}(k_1 - ik_2) + a^1_{-ki\alpha}a^1_{kj\beta}(k_1 + ik_2) \\ &- 2a^1_{-ki\alpha}a^2_{kj\beta}k_3] \\ \rightarrow\ &\frac{1}{E}[a^2_{ki\alpha}a^2_{-kj\beta}(k_1 - ik_2) \\ &- a^1_{ki\alpha}a^1_{-kj\beta}(k_1 + ik_2) + 2a^2_{ki\alpha}a^1_{-kj\beta}k_3], \end{aligned} \tag{C6}$$

where we have relabeled $k \rightarrow -k$, $i \leftrightarrow j$, $\alpha \leftrightarrow \beta$ in the last line. The final result is a sum over k,α,β,i,j of

$$\begin{aligned} \frac{2}{E}[&a^2_{ki\alpha}a^2_{-kj\beta}(k_1 - ik_2) - a^1_{ki\alpha}a^1_{-kj\beta}(k_1 + ik_2) \\ &+ (a^1_{ki\alpha}a^2_{-kj\beta} + a^2_{ki\alpha}a^1_{-kj\beta})k_3]. \end{aligned} \tag{C7}$$

Upon inserting the relevant spherical harmonics and using standard arrow notation for the spins we obtain

$$\begin{aligned} \psi C\mathcal{S}\psi \rightarrow -2\sqrt{8\pi}\frac{p}{E}\Bigg[&\frac{1}{\sqrt{3}}|\uparrow\uparrow\rangle Y_1^{-1} + \frac{1}{\sqrt{3}}|\downarrow\downarrow\rangle Y_1^1 \\ &- \frac{1}{\sqrt{3}}\frac{1}{\sqrt{2}}[|\uparrow\downarrow\rangle + |\downarrow\uparrow\rangle]\Bigg] Y_1^0, \end{aligned} \tag{C8}$$

which has precisely the correct Clebsch-Gordan structure to be interpreted as a state with orbital angular momentum $l=1$, which gives an antisymmetric spatial wave function, and spin $s=1$, which gives a symmetric spin wave function, combined to give $j=0$. We write this as $|l=1_A, s=1_S\rangle$. Applying this to all the condensates we studied, we can make a table of the particle-particle (as opposed to particle-hole) content of each of them:

$$\psi C\gamma_5\mathcal{S}\psi\text{:}\quad 4\sqrt{2\pi}|l=0_S, s=0_A\rangle, \tag{C9}$$

$$\psi C\mathcal{S}\psi\text{:}\quad -2\sqrt{8\pi}\frac{p}{E}|l=1_A, s=1_S\rangle,$$

$$\psi C\gamma_0\gamma_5\mathcal{S}\psi\text{:}\quad 4\sqrt{2\pi}\frac{m}{E}|l=0_S, s=0_A\rangle,$$

$$\psi C\gamma_3\gamma_5\mathcal{S}\psi\text{:}\quad 8\sqrt{\frac{\pi}{3}}\frac{p}{E}|l=1_A, s=1_S\rangle,$$

$$\psi C\sigma_{03}\gamma_5\mathcal{A}\psi\text{:}\quad -4i\sqrt{\frac{2\pi}{3}}\frac{p}{E}|l=1_A, s=0_A\rangle,$$

$$\psi C\sigma_{03}\mathcal{A}\psi\text{:}\quad \begin{cases} -\frac{8}{3}\sqrt{\pi}i\,\frac{p^2}{E(E+m)}|l=2_S, s=1_S\rangle, \\ +2i\sqrt{2\pi}\left[\frac{(E+m)^2 - \frac{1}{3}p^2}{E(E+m)}\right]|l=0_S, s=1_S\rangle, \end{cases}$$

$$\psi C\gamma_0\mathcal{A}\psi\text{:}\quad 0,$$

$$\psi C\gamma_3 \mathcal{A}\psi: \quad \begin{cases} \frac{8}{3}\sqrt{\pi}\,\frac{p^2}{E(E+m)}|l=2_S, s=1_S\rangle, \\ +2\sqrt{2\pi}\left[\frac{(E+m)^2-\frac{1}{3}p^2}{E(E+m)}\right]|l=0_S, s=1_S\rangle. \end{cases}$$

These results are summarized in the ''BCS-enhanced'' column of Table I. We can see explicitly that the $\psi C\gamma_0\gamma_5\psi$ condensate has no particle-particle component in the massless limit, which is why it cannot occur at high density for the up and down quarks. This reflects basic physics: the condensate has spin zero, so the two spins must be oppositely aligned. But it is an LR condensate (see Table I), so in the massless limit the two quarks, having opposite momentum and opposite helicity, have parallel spins.

[1] B. Barrois, Nucl. Phys. **B129**, 390 (1977); S. Frautschi, in Proceedings of Workshop on Hadronic Matter at Extreme Density, Erice, 1978.

[2] D. Bailin and A. Love, Phys. Rep. **107**, 325 (1984), and references therein.

[3] M. Iwasaki and T. Iwado, Phys. Lett. B **350**, 163 (1995); M. Iwasaki, Prog. Theor. Phys. Suppl. **120**, 187 (1995).

[4] M. Alford, K. Rajagopal, and F. Wilczek, Phys. Lett. B **422**, 247 (1998).

[5] R. Rapp, T. Schäfer, E. V. Shuryak, and M. Velkovsky, Phys. Rev. Lett. **81**, 53 (1998).

[6] M. G. Alford, Annu. Rev. Nucl. Part. Sci. **51**, 131 (2001); K. Rajagopal and F. Wilczek, hep-ph/0011333; T. Schäfer and E. V. Shuryak, in *Physics of Neutron Star Interiors*, Lecture Notes in Physics Vol. 578, edited by D. Blaschke, N. Glendenning, and A. Sedrakian (Springer, Berlin, 2001), p. 203, nucl-th/0010049; D. K. Hong, Acta Phys. Pol. B **32**, 1253 (2001); S. D. Hsu, hep-ph/0003140; D. H. Rischke and R. D. Pisarski, nucl-th/0004016.

[7] M. Alford, K. Rajagopal, and F. Wilczek, Nucl. Phys. **B537**, 443 (1999).

[8] J. Bardeen, L. Cooper, and J. Schrieffer, Phys. Rev. **106**, 162 (1957); **108**, 1175 (1957).

[9] G. Carter, D. Diakonov, Phys. Rev. D **60**, 016004 (1999).

[10] J. Berges and K. Rajagopal, Nucl. Phys. **B538**, 215 (1999).

[11] T. M. Schwarz, S. P. Klevansky, and G. Papp, Phys. Rev. C **60**, 055205 (1999); B. Vanderheyden and A. D. Jackson, Phys. Rev. D **62**, 094010 (2000); F. Gastineau, R. Nebauer, and J. Aichelin, Phys. Rev. C **65**, 045204 (2002); B. O. Kerbikov, hep-ph/0106324; M. Huang, P. F. Zhuang, and W. Q. Chao, Phys. Rev. D **65**, 076012 (2002).

[12] M. Oertel and M. Buballa, hep-ph/0202098; M. Boballa and M. Oertel, Nucl. Phys. **A703**, 770 (2002).

[13] S. Hands and D. N. Walters, Phys. Lett. B **548**, 196 (2002).

[14] D. Son, Phys. Rev. D **59**, 094019 (1999).

[15] T. Schäfer and F. Wilczek, Phys. Rev. D **60**, 114033 (1999); R. Pisarski and D. Rischke, *ibid.* **61**, 074017 (2000); D. Hong, Nucl. Phys. **B582**, 451 (2000); Phys. Lett. B **473**, 118 (2000); R. Pisarski and D. Rischke, Phys. Rev. D **61**, 051501(R) (2000); D. Hong, V. Miransky, I. Shovkovy, and L. Wijewardhana, *ibid.* **61**, 056001 (2000); **62**, 059903(E) (2000); S. Hsu and M. Schwetz, Nucl. Phys. **B572**, 211 (2000).

[16] W. Brown, J. Liu, and H. Ren, Phys. Rev. D **61**, 114012 (2000); **62**, 054016 (2000); **62**, 054013 (2000).

[17] T. Schäfer, Nucl. Phys. **B575**, 269 (2000).

[18] I. Shovkovy and L. Wijewardhana, Phys. Lett. B **470**, 189 (1999).

[19] M. Alford and K. Rajagopal, J. High Energy Phys. **06**, 031 (2002).

[20] A. W. Steiner, S. Reddy, and M. Prakash, Phys. Rev. D **66**, 094007 (2002).

[21] T. Schafer and F. Wilczek, Phys. Rev. D **60**, 074014 (1999).

[22] M. Alford, hep-ph/0110150.

[23] P. F. Bedaque and T. Schäfer, Nucl. Phys. **A697**, 802 (2002).

[24] T. Schäfer, Phys. Rev. D **65**, 094033 (2002).

[25] A. I. Larkin and Yu. N. Ovchinnikov, Zh. Eksp. Teor. Fiz. **47**, 1136 (1964) [Sov. Phys. JETP **20**, 762 (1965)]; P. Fulde and R. A. Ferrell, Phys. Rev. **135**, A550 (1964).

[26] M. Alford, J. Bowers, and K. Rajagopal, Phys. Rev. D **63**, 074016 (2001).

[27] J. A. Bowers and K. Rajagopal, Phys. Rev. D **66**, 065002 (2002).

[28] T. Schäfer, Phys. Rev. D **62**, 094007 (2000).

[29] M. Buballa, J. Hosek, and M. Oertel, hep-ph/0204275.

[30] C. Wetterich, Phys. Rev. D **64**, 036003 (2001); J. Berges and C. Wetterich, Phys. Lett. B **512**, 85 (2001).

[31] B. Barrois, Ph.D. thesis, Cal Tech, Report No. UMI 79-04847-mc, 1979.

[32] N. K. Glendenning, Phys. Rev. D **46**, 1274 (1992); *Compact Stars* (Springer-Verlag, Berlin, 1997); F. Weber, J. Phys. G **25**, R195 (1999).

[33] A. Schmitt, Q. Wang, and D. H. Rischke, Phys. Rev. D **66**, 114010 (2002).

[34] M. Alford, J. Berges, and K. Rajagopal, Nucl. Phys. **B558**, 219 (1999).

[35] T. D. Fugleberg, hep-ph/0206033.

[36] R. D. Pisarski and D. H. Rischke, nucl-th/9907094.

[37] J. Berges, Phys. Rev. D **64**, 014010 (2001).

[38] C. Wetterich, Phys. Lett. B **525**, 277 (2002).